NASA

NEUTRON AND ANTINEUTRON PRODUCTION IN ACCRETION ONTO COMPACT OBJECTS

CHARLES D. DERMER

REUVEN RAMATY

LABORATORY FOR HIGH ENERGY ASTROPHYSICS

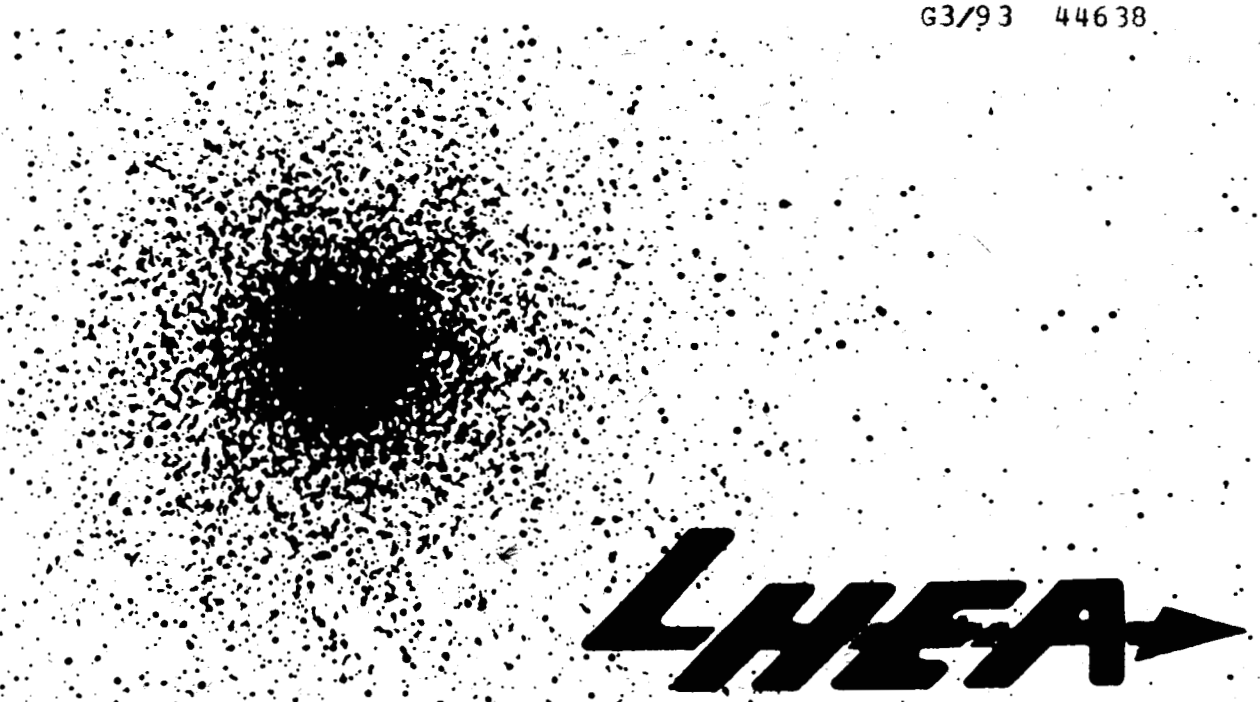

LHEA

National Aeronautics And Space Administration

Goddard Space Flight Center

Greenbelt, Maryland 20771

86-012

NEUTRON AND ANTINEUTRON PRODUCTION IN ACCRETION ONTO COMPACT OBJECTS

Charles D. Dermer and Reuven Ramaty
Laboratory for High Energy Astrophysics
NASA/Goddard Space Flight Center
Greenbelt, MD 20771, U.S.A.

JULY 1986

To appear in the Proceedings of the VIth Moriond Astrophysics Meeting

NEUTRON AND ANTINEUTRON PRODUCTION IN ACCRETION ONTO COMPACT OBJECTS

Charles D. Dermer[1] and Reuven Ramaty
NASA/Goddard Space Flight Center
Greenbelt, MD 20771, U.S.A.

ABSTRACT

Nuclear reactions in the hot accretion plasma surrounding a collapsed star are a source of neutrons, primarily through spallation and pion-producing reactions, and antineutrons, principally through the reaction $p+p \rightarrow p+p+n+\bar{n}$. We calculate spectra of neutrons and antineutrons produced by a variety of nonthermal energetic particle distributions in which the target particles are either at rest or in motion. If only neutral particles are free to escape the interaction site, a component of the proton and antiproton fluxes in the cosmic radiation results from the neutrons and antineutrons which leave the accretion plasma and subsequently decay in the interstellar medium. This additional antiproton component could account for the enhanced flux of antiprotons in the cosmic radiation, compared to values expected from the standard "leaky-box" model of cosmic-ray propagation and confinement. Moreover, the low-energy antiproton flux measured by Buffington et al. (1981) could result from target-particle motion in the accretion plasma. This model for the origin of antiprotons predicts a narrow 2.223 MeV line which could be observable.

[1]NAS/NRC Resident Research Associate

INTRODUCTION

Matter accreting onto collapsed objects can attain very high energies due to the conversion of gravitational energy into kinetic energy. Because of thermal decoupling of the electrons and ions in accreting thermal plasma, the ion component may reach temperatures in excess of 100 MeV in disk (e.g., Shapiro, Lightman and Eardley 1976; Eilek and Kafatos 1983) and spherical accretion models (e.g., Dahlbacka, Chapline and Weaver 1974; Kolykhalov and Sunyaev 1979; Meszaros and Ostriker 1983). Neutrons are formed in a hot accretion plasma through nuclear breakdown reactions at temperatures $\gtrsim$ 1 MeV (Aharonian and Sunyaev 1984; Gould 1986) and in association with pion-producing reactions (Dermer 1986) at temperatures $\gtrsim$ 20 MeV. At temperatures $\gtrsim$ 200 MeV, a channel of neutron and antineutron production is opened through the reaction $p + p \rightarrow p + p + n + \bar{n}$ which, moreover, produces a spectrum of antineutrons extending to low energies (Dermer and Ramaty 1986), in contrast to the spectrum of antineutrons produced in collisions of protons with a stationary target (e.g., Stephens 1981). These neutrons and antineutrons, unconfined by the magnetic field of the accretion plasma, can escape into the interstellar medium and, after decaying, be detected as a low energy proton and antiproton component of the cosmic radiation.

Support for thermal accretion models of galactic X-ray sources is provided particularly by the case of Cyg X-1, whose X-ray spectrum is successfully fit using either disk (Shapiro, Lightman and Eardley 1976) or spherical (Meszaros 1983) accretion geometries. But the existence of galactic point sources emitting gamma radiation at energies $\varepsilon > 10^{12}$ eV implies that energetic nonthermal particle spectra are common in galactic binary X-ray sources such as Cyg X-3 and Her X-1. Particle acceleration in confined volumes, with maximum sizes inferred from time-variability arguments, requires intense magnetic fields (Hillas 1984a). Only charged particles with energy $E(\mathrm{GeV}) \gtrsim 90 Z B_3 M_0$, where B_3 is the magnetic field at the interaction site in units of 10^3 gauss, M_0 is the mass of the collapsed object in solar masses and Ze is the charge of the ion, can directly escape from the interaction region, assuming that the gyroradius must approximately equal the Schwarzschild radius for charged-particle escape. Neutrons and antineutrons, on the other hand, leave the interaction region directly provided that (i) the mass of the collapsed object is $< 10^7\ M_0$ (Dermer and Ramaty 1986), (ii) the grammage shrouding the interaction region is $\lesssim$ 50 gm/cm^2, and (iii) $\mu \cdot \partial B/dx \approx$

$10^{-23}B_3/M_0 < E(GeV)$, where μ is the magnetic dipole moment of the neutron. These conditions ensure that the neutrons or antineutrons (i) do not decay before escape, (ii) do not interact strongly before escape, and (iii) do not significantly change energy when traversing the intense, turbulent magnetic field likely to be found in the accreting plasma. Condition (iii) is easily satisfied even if the correct distance scale for magnetic field variation is much smaller than the Schwarzschild radius used in this estimate. The other conditions are also not difficult to satisfy in galactic sources.

In this paper, we calculate the spectra of neutrons and antineutrons produced by energetic nonthermal particle distributions located in the vicinity of a compact object. We do not consider the detailed nature of the acceleration mechanism and interaction site, but for simplicity assume an isotropic, energetic particle distribution of solar (photospheric) composition. We consider two interaction models which take into account the trapping of the charged particles in the interaction region. In the first, the particles are assumed to interact with an ambient background plasma in the thick-target model (e. g., Ramaty, Kozlovsky and Lingenfelter 1975). This model has been extensively developed to interpret gamma-ray and neutron observations from solar flares (Murphy and Ramaty 1985, and references therein). In the second, the energetic particles interact only with each other, that is, we consider a relativistic nonthermal plasma. We employ shock-acceleration spectra with a spectral index ~2.2 appropriate to the cosmic radiation before effects of the energy-dependent escape are taken into account. This source could account for the antiprotons observed in the cosmic radiation (Golden et al. 1979; Bogomolov et al. 1979; Buffington et al. 1981) in excess of the leaky-box model prediction. A narrow 2.223 MeV line due to the energetic neutrons thermalizing and being captured by protons in the atmosphere of a binary stellar companion might also be formed.

ANALYSIS

In the thick-target model, the interacting primary and secondary energetic charged particles remain trapped in the interaction region and lose energy through particle collisions with the ambient plasma, while the neutral particles are free to escape. The spectrum of the antineutrons injected into the interstellar medium is identical to the spectrum at production under the conditions listed in the Introduction, except for a possible gravitational

redshifting. Neglecting this last complication, the source spectrum of antineutrons (particle 3) produced in the reaction 1 + 2 → 3 + X is just

$$\dot{n}_3(E_3)\ [cm^{-3}\text{-}s^{-1}\text{-}GeV^{-1}] = 4\pi n_1 \int_{E_2^{min}(E_3)}^{\infty} dE_2 \cdot J_2(E_2) \cdot \frac{d\sigma_{1+2\to 3+X}(E_3;E_2)}{dE_3}\ , \qquad (1)$$

where n_1 is the ambient target particle density, $J_2(E_2)$ is the equilibrium flux of energetic particle species 2, including secondaries, $E_2^{min}(E_3)$ is the minimum energy of a particle of type 2 necessary to produce particle 3 with energy E_3, and $d\sigma_{1+2\to 3+X}(E_3;E_2)/dE_2$ is the differential cross section for the production of particle 3 with energy E_3 in a collision between particle 2, with energy E_2, and stationary particle 1. The flux $[cm^{-2}\text{-}s^{-1}\text{-}sr^{-1}\text{-}GeV^{-1}]$

$$J_2(E_2) = [4\pi m_p n_1 |\frac{dE_2}{d\Lambda}|]^{-1} \int_{E_2}^{\infty} dE_2' \cdot \dot{n}_2(E_2') \cdot \exp\{-\int_{E_2}^{E_2'} dE''/[\Lambda_{12}(E'') \cdot |\frac{dE_2}{d\Lambda}|]\}, \qquad (2)$$

where $\dot{n}_2(E_2)$ is the rate at which particles of type 2 are injected per cm^3 per GeV, and $dE_2(E_2)/d\Lambda$ is the rate at which they lose energy per unit grammage traversed. Nuclear collisions are treated as a particle sink in terms of the grammage $\Lambda_{12}(E_2) \approx m_p/\sigma_{12}(E_2)$, in which case secondaries particles must be added explicitly in the term $\dot{n}_2(E_2)$ (see below).

In a relativistic plasma, the energetic particle density is sufficiently great that reactions of particles in motion with other particles in motion dominates secondary production. A relativistically correct description of the reaction rate for producing particles of type 3 in reactions of particles of type 1 and 2 is given by

$$Q_3[cm^{-3}\text{-}s^{-1}] = \tfrac{1}{2}(1+\delta_{12})^{-1} c \int_0^{\infty} dp_1 F_1(p_1) \int_0^{\infty} dp_2 F_2(p_2) \int_{-1}^{+1} d\cos\theta \cdot \beta_r \cdot (1-\beta_1\beta_2\cos\theta)$$
$$\times \int_{m_3}^{E^*_{max,3}} dE^* \int_{-1}^{+1} d\mu^* \frac{d^2\sigma^*_{1+2\to 3+X}(E^*,\mu^*;\gamma_r)}{dE^* d\mu^*} \qquad (3)$$

(cf. Dermer 1984). In this equation,

$$n_i = \int_0^{\infty} dp_i F_i(p_i)\ ,\ i=1,2 \qquad (4)$$

is the density, $F_i(p_i)$ is the isotropic differential momentum spectrum, and

$p_i=m_i\beta_i\gamma_i$ is the momentum variable of particles of type i. The term $E^*_{max,3}$ is the maximum CMS energy of particle 3 and is a function of the relative Lorentz factor $\gamma_r=(E_1E_2-p_1p_2\cos\theta)/m_1m_2$ only, where E_1 and E_2 are the energies of the colliding particles and θ is the angle between their directions of motion in the LS. The CMS differential cross section for the production of particle 3 in terms of CMS energy E* and CMS angle $\theta^*=\cos^{-1}\mu^*$ is denoted by $d^2\sigma^*/dE^*d\mu^*$.

We employ nonthermal energetic particle spectra predicted by shock acceleration theory. The momentum spectrum resulting from diffusive shock acceleration is given by $F_i(p_i) \propto p_i^{-q}$ (e.g., Blandford and Ostriker 1978). Normalizing this spectrum using equation (4) gives

$$n_i = K_i\int_{p_{co,i}}^{\infty} dp_i\cdot p_i^{-q} \ , \quad i=1,2, \tag{5}$$

where K_i is the normalization constant, n_i is the volume density, and $p_{co,i}$ is the low-momentum cutoff in the momentum spectrum of particles of type i.

We solve equation (3) using the Monte-Carlo method, generalizing the technique of Ramaty and Meszaros (1981) to secondary particles created in the collisions of particles with, in general, different masses. Introduce an array of six numbers chosen randomly between 0 and 1, namely $r_1,\ldots,r_6$. Choose values of momenta p_1 and p_2 from the inverted particle distribution functions. The shock spectrum can be analytically inverted, giving

$$p_i = p_{co,i}\cdot r_i^{\left(\frac{1}{1-q}\right)} \ , \quad i=1,2. \tag{6}$$

Choose the remaining variables from uniform distributions: $\cos\theta=2r_3-1$, $E^* = m_3+[E^*_{max,3}(\gamma_r)-m_3]\cdot r_4$, $\mu^*=2r_5-1$ and $\phi^*=2\pi r_6$, where ϕ^* is the CMS azimuthal angle of the outgoing particle of mass m_3. The reaction rate (3) is then given by

$$Q_3 = \frac{\frac{1}{2}n_1n_2c}{N_{tot}(1+\delta_{12})}\sum_{i=1}^{N_{tot}}\left(\frac{2\beta_r\gamma_r}{\gamma_1\gamma_2}\right)\cdot[E^*_{max,3}(\gamma_r)-m_3]\cdot 2\cdot\frac{d^2\sigma^*}{dE^*d\mu^*} \tag{7}$$

in the limit N_{tot}, the number of Monte-Carlo trials, goes to infinity. Differential energy spectra are determined by calculating differential reaction probabilities from the individual Monte-Carlo trials of equation (7)

and binning in energy. The energy of particle 3, E_3, was determined from the kinematical relations $E_3 = \gamma_c(E_3^*+\beta_c p_3^*\cos\theta^*)$, where $\gamma_c = (\gamma_1+\gamma_2)/s^{\frac{1}{2}}$, $s = m_1^2+m_2^2+2m_1m_2\gamma_r$, and $\cos\theta^* = \mu^*\eta^*+(1-\mu^{*2})^{\frac{1}{2}}\cdot(1-\eta^{*2})^{\frac{1}{2}}\cdot\cos\phi^*$, where $\eta^* = (E_1-\gamma_c E_1^*)/\beta_c\gamma_c p_1^*$ and $E_1^* = (s+m_1^2-m_2^2)/2s^{\frac{1}{2}}$. In the limit $\gamma_2\to 1$, that is, $F(p_2) \to \delta(p_2)$, equations (3) and (7) reduce to the stationary target case.

NUMERICAL RESULTS

A detailed description of the cross sections and energy spectra for the production of secondary neutrons and protons in reactions involving protons and α particles is given by Murphy, Dermer and Ramaty (1987). A description of secondary neutron production in collisions involving heavier nuclei will be given elsewhere. A complete version of the calculations relevant to this work is in preparation.

For calculations of neutron and antineutron production in a thick target, we assume solar composition (Cameron 1982) for the ambient plasma and the energetic particles, that is, the number of particles with energy greater than 30 MeV/nucleon is assumed proportional to the Cameron abundance of that species. Calculations of secondary proton and neutron production at energies $\lesssim$ 5 GeV/nucleon involve integrations over complicated secondary energy spectra and cross sections and were evaluated from equations (1) and (2) using a Monte Carlo simulation (cf. Murphy 1985). At energies $\gtrsim$ 5 GeV, the effects of α particles and heavy nuclei can be treated as a multiplicative correction to the basic proton-proton (p-p) reactions. Taking $\Lambda_{p-p} \approx 50$ gm/cm^2 and $|dE_p/d\Lambda| \approx 4\times10^{-3}$ GeV/(gm/cm^2) (Murphy 1985) in equation (2) gives a simple 1-dimensional integral for the thick-target equilibrium proton flux. Using this flux, we calculated the injection sources of antineutrons and $\gtrsim$ 5 GeV neutrons from equation (1) using the scaling representations of Tan and Ng (1983a; see Murphy, Dermer and Ramaty 1987).

In the calculations of neutron and antineutron production in a relativistic plasma, we assume that there is 1 proton per cm^3 with momentum greater than the low-momentum cutoff, and that the number of energetic particles above the cutoff momentum is proportional to the Cameron abundance of that species. If the low-momentum cutoff $p_{co,i}$ tends to zero, interactions

of the energetic particles with particles nearly at rest dominate secondary production because of the divergence in the normalization of the shock spectrum in this limit [see eq. (5)]. The problem therefore reduces to a thin-target calculation. As $p_{co,i}$ becomes large, the average collision energy increases, and reactions of particles in motion with other particles in motion becomes more probable. Due to the large antineutron production threshold, the effect of increasing $p_{co,i}$ causes the relative production of antineutrons compared to neutrons to increase. Also, the spectrum of antineutrons now extends to low energy, as most $\bar{n}$ are formed with low energy in the CMS of the colliding protons, and the CMS can now have low velocity in the rest frame of the plasma (Dermer and Ramaty 1986).

We consider neutron and antineutron production in a relativistic plasma using a specific model with $p_{co,i} = p_{co}$ =500 MeV/c for all i. A low-momentum cutoff of 500 MeV/c corresponds to a low-energy cutoff of ~125 MeV for the protons. We find that for these parameters and normalizations, the integrated production rates of neutrons and antineutrons are 3.2×10^{-16} cm^{-3}-s^{-1} and 5.5×10^{-19} cm^{-3}-s^{-1}, respectively. This implies that ~580 neutrons are produced for each antineutron.

OBSERVABLE CONSEQUENCES

A review of the cosmic ray antiproton observations and models is given by Golden (1984), and the measured fluxes of antiprotons in the cosmic radiation are shown in Fig. 1. The prediction of the leaky-box model (Tan and Ng 1983b), in which cosmic rays traverse an energy-dependent average grammage before escaping from the galaxy, is also shown here. This model fails by about three to five to account for the measurements between 2 and 10 GeV. It fails by over an order-of-magnitude to explain the low-energy measurement of Buffington et al. (1981), even if the effects of the solar modulation of cosmic-ray protons and antiprotons are taken into account (Tan and Ng 1983b).

We propose that the antiprotons in the cosmic radiation in excess of the leaky box contribution have their origin in additional discrete galactic sources which produce antineutrons through nuclear reactions in an accretion plasma. The production of antiprotons through secondary collisions is suggested by the lack of observations of A > 1 antinuclei, whose production in collisions of normal matter particles is negligible. This argues in favor of

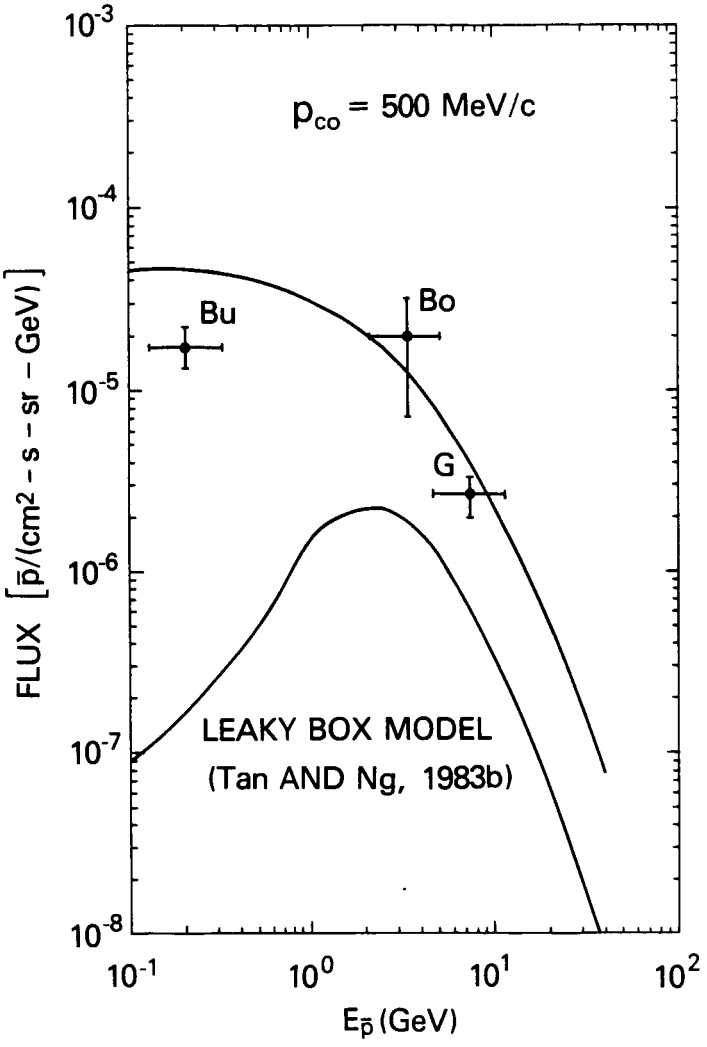

Fig. 1. The observed cosmic-ray antiproton fluxes, shown by the data points, are designated by Bu (Buffington, et al. 1981), Bo (Bogomolov, et al. 1979), and G (Golden et al., 1979). The lower curve gives the leaky-box model prediction of Tan and Ng (1983b) and the upper curve is the antiproton flux resulting from the decay of antineutrons produced in a nonthermal relativistic plasma with p_{co} = 500 MeV/c. This flux is fit to the antiproton data in excess of the leaky-box model contribution.

an additional secondary source of antiprotons. Low-energy antiprotons are produced in relativistic plasmas as a direct consequence of the kinematics of such systems, and these plasmas could be formed in the vicinity of a compact object. The associated production of neutrons is a necessary consequence of this model, and suggests a potentially observable signature, which we discuss below.

The antiproton flux resulting from the decay of antineutrons produced in a relativistic plasma with p_{co} = 500 MeV/c and normalized to the data is shown in Fig. 1. The galactic antiproton flux was evaluated from the antineutron source spectra using the relation

$$J_{\bar{p}}(E_{\bar{p}}) = \eta \cdot \frac{\dot{n}_{\bar{n}}(E_{\bar{n}})}{4\pi n_G} \cdot \left(\frac{m_p}{\Lambda_{esc}} + \sigma_{\bar{p}}^{inel}\right)^{-1} , \qquad (8)$$

where n_G [cm^{-3}] is the average proton density in the galaxy. The parameters describing the average grammage traversal Λ_{esc} and the antiproton inelastic cross section $\sigma_{\bar{p}}^{inel}$ are given by Tan and Ng (1983b). The effects of ionization energy loss and reinjection of antiprotons following non-annihilation inelastic interactions are unimportant for this source spectrum and are neglected. The constant η in equation (8) was chosen to give the proper source strength to account for the observed antiproton observations. We obtain a total galactic antineutron production rate of $\sim 1.3 \times 10^{39} V_{67} n_{0.2}$ antineutrons per second for this model, where V_{67} is the volume of the Galaxy in units of 10^{67} cm^3 and $n_{0.2}$ is the average galactic proton density in units of 0.2 protons per cm^3. From Fig. 1 we see that the combined source of antiprotons resulting from this model and the leaky-box model gives an adequate representation of the data above 2 GeV. There is also a substantial flux of low energy antiprotons produced in this model, which might be sufficient to account for the low-energy measurement of Buffington et al. (1983), depending on the uncertain degree of solar modulation occurring during this period of observation.

The value of η chosen to fit the cosmic-ray antiproton observations implies a related proton flux from neutron decay. We have evaluated this flux from the neutron source spectrum associated with the antineutron source spectrum, but now with $\sigma_{\bar{p}}^{inel}$ in equation (8) replaced by the proton-proton inelastic cross section. The result is compared in Fig. 2 to the observed cosmic ray proton flux (data referenced in Gloeckler and Jokipii 1967 and Tan and Ng 1983b). As can be seen, the neutron-decay proton flux implied by this model does not conflict with the observed protons in the cosmic radiation. Above several GeV, these protons comprise about 10% of the observed cosmic-ray protons. At lower energies this source appears to contribute a larger percentage, but the effects of solar modulation will lower the calculated flux at these energies. The total galactic neutron production corresponding to the antineutron flux of Fig. 1 is $\sim 7.5 \times 10^{41} V_{67} n_{0.2}$ neutrons per second.

Antineutrons and neutrons escaping from the interaction region either decay in interstellar space or are captured or annihilate in a dense medium, such as the atmosphere of a star. In the first case, positrons and electrons are formed in the decay of the antineutrons and neutrons, but represent negligible additions to the electron and positron fluxes of the cosmic

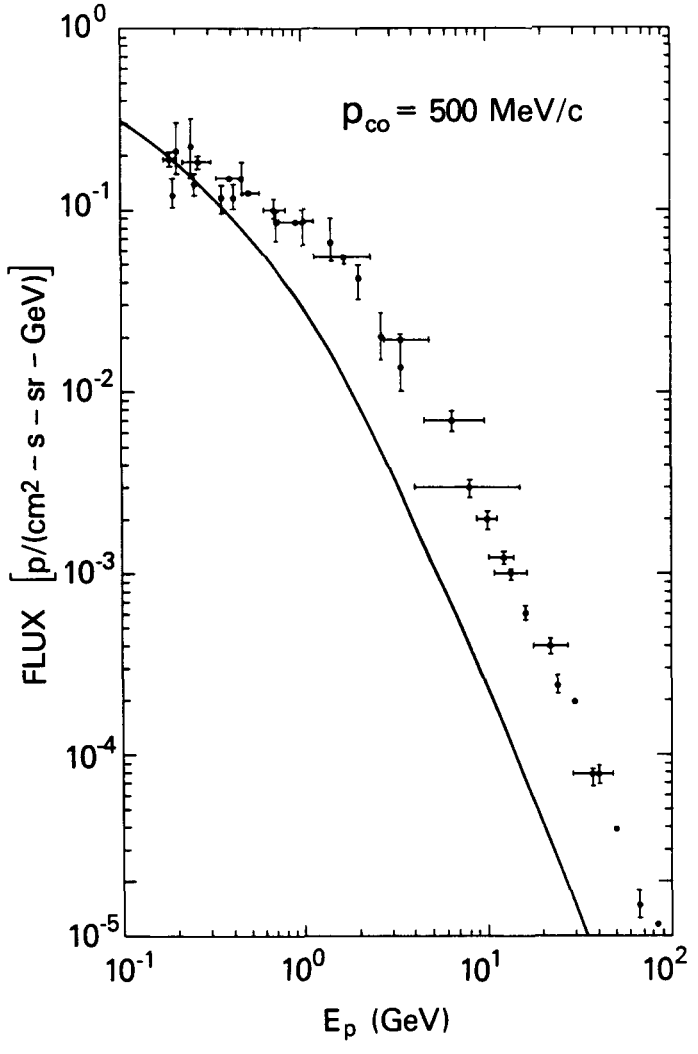

Fig. 2. The data points give the observed solar minimum cosmic-ray proton fluxes (see Jokipii and Gloeckler 1967 and Tan and Ng 1983b). The solid curve represents the interstellar neutron-decay proton flux produced in association with the antiproton flux of Fig. 1.

radiation due to the relatively small Lorentz factors and intensities of the neutron and antineutron source functions. An inner bremmstrahlung (Petrosian and Ramaty 1972) X-ray emissivity from the decay of the neutral particles is also produced at a level of $\sim \alpha \cdot 0.5$ MeV/n $\cdot\ 10^{42}$ n/s $\sim 6 \times 10^{33}$ ergs/s, where α is the fine structure constant. This represents a weak X-ray luminosity, even if concentrated in a single source.

The capture of the neutrons and antineutrons is possible if, for example, the compact object is accompanied by a binary companion which subtends a significant solid angle about the interaction region. This companion star could also be the source of the accretion plasma that powers the system. Neutrons impinging on the atmosphere of the star would thermalize and, depending on the ^{3}He content of the stellar atmosphere, produce deuterium in the capture reaction $n + p \rightarrow {}^2H + \gamma(2.223\ \text{MeV})$, as in the case of solar flares (Wang and Ramaty 1974). If all neutrons are captured and produce deuterium,

this represents a production rate of ~3×10^{17}sec · 10^{42}n/s ~ 3×10^{59} ^{2}H produced during the age of the galaxy. This can be compared to a value of ~$1.2\times10^{63}c_{-5}$ deuterons in the galaxy, where c_{-5} is the relative deuterium-to-hydrogen galactic abundance in units of 10^{-5}. This source obviously does not conflict with the observed galactic ^{2}H abundance, but neither does it significantly contribute to it.

The formation of a deuteron is accompanied by the production of a 2.223 MeV gamma ray. For solar flares, where this effect is clearly seen, approximately 0.1 line photons are produced per neutron (Murphy and Ramaty 1985). Let $0.1f_{-1}$ be a numerical factor reflecting the probability that for each neutron formed in the accretion plasma, a 2.223 MeV photon is emitted into interstellar space. This factor incorporates a number of uncertain factors including the solid angle of the companion star and the probability that the gamma ray is both produced and able to leave the stellar atmosphere without being absorbed. We therefore have that ~ $7.5\times10^{40}f_{-1}V_{67}n_{0.2}$ line photons per second are produced in the galaxy. If there are a large number of sources distributed in the galaxy, this represents a flux observed at Earth of ~ $10^{-5}f_{-1}V_{67}n_{0.2}$ photons/(cm^2-s-rad), normalizing to the observed flux of 1.809 MeV photons from ^{26}Al decay (i.e., 3 $M_\odot$ of ^{26}Al with a mean life $\tau_{^{26}Al}$ ~ 1.1×10^6 yr produce about 5×10^{-4} photons-cm^{-2}-s^{-1}-rad^{-1} [Mahoney et al. 1984]).

If the number of discrete sources is small, then the 2.223 MeV line flux could be observed from a single object. Taking the number of sources in the galaxy to be $10N_{10}$, the flux of 2.223 MeV photons observed at Earth from a single source is ~ $6\times10^{-7}f_{-1}V_{67}n_{0.2}/(N_{10}r_{10}^2)$ photons/(cm^2-s), where r_{10} is the distance of the source to the Earth in units of 10 kpc. The detection of the line flux would be aided by the fact that the line intensity will vary with the underlying binary period of the system. In addition, since this estimate is based on the average source luminosity over the age of the cosmic rays, a temporary outburst could increase the emission expected from a single source. Likely candidates for observation include the binary X-ray sources listed in the Introduction, whose ultra-high-energy gamma-ray flux is evidently powered by an accretion mechanism, perhaps in association with a neutron star. A current interpretation of the origin of the high-energy gamma-ray flux pictures energetic hadrons emerging from the compact object and impinging upon the atmosphere of a companion star (e.g., Berezinsky 1977;

Vestrand and Eichler 1982; Hillas 1984b; Kazanas and Ellison 1986). The observation of a 2.223 MeV signal in the transient event of 10 June 1974 (Jacobson et al. 1978; Ling et al. 1982) is perhaps an example of this type of source, although with nonsteady accretion.

CONCLUSIONS

We have presented the physics of secondary neutron and antineutron production from particle collisions in a thick target and in a nonthermal relativistic plasma. Because the neutrons and antineutrons are not confined by the magnetic field of the accretion plasma, they can leave the interaction site and either decay in interstellar space or be captured on a companion star. Assuming that most of the neutral particles decay in interstellar space, we have fit the spectrum of secondary antineutrons to the observed cosmic ray antiproton flux, using a relativistic plasma with a low-momentum cutoff of 500 MeV/c and taking into account the leaky-box contribution of antiprotons. This normalization implies a production rate of about 10^{42} neutrons per second in the galaxy. This level of production does not violate the deuterium content of the galaxy and provides only a weak X-ray source resulting from inner bremsstrahlung in neutron decay. If about one 2.223 MeV gamma-ray photon is emitted into interstellar space for every 10 neutrons formed, for example by neutron capture on protons in the atmosphere of a stellar companion of the compact object, a flux of line photons of $\sim 10^{-5}$ photons/(cm^2-s-rad) could result from distributed sources in the galaxy. A gamma-ray line flux at 2.223 MeV might be observable from discrete sources depending on source luminosity, distance and duration of the active phase. Detection of this line could be facilitated by the variation of the flux with the period of the binary system.

ACKNOWLEDGEMENTS

C.D.D. would like to acknowledge the suggestion of C. J. Cesarsky to calculate the joint neutron and antineutron production in compact sources. We also acknowledge useful discussions with R. J. Murphy and D. Kazanas.

REFERENCES

Aharonian, F. A., and Sunyaev, R. A. 1984, M.N.R.A.S., **210**, 257.

Berezinsky, V. S. 1980, Proc. 1979 DUMAND Summer Workshop at Khabarovsk and Lake Baikal, ed. J. G. Learned, U. Hawaii Press, p. 245.

Blandford, R. D., and Ostriker, J. P. 1978, Ap. J., **221**, L29.

Bogomolov, E. A., Lubyananya, N. D., Romanov, V. A., Stepanov, S. V., Shulkova, M. S. 1979, Proc. 16th ICRC, (Kyoto), **1**, 330.

Buffington, A., Schindler, S. M., and Pennypacker, C. R. 1981, Ap. J., **248**, 1179.

Cameron, A. G. W. 1982, in Essays in Nuclear Astrophysics, ed. C. Barnes, D. D. Clayton, and D. N. Schramm (Cambridge University Press: Cambridge), p. 23.

Dahlbacka, G. H., Chapline, G. F., and Weaver, T. A. 1974, Nature, **250**, 36.

Dermer, C. D. 1984, Ap. J., **280**, 328.

Dermer, C. D. 1986, Ap. J., in press.

Dermer, C. D., and Ramaty, R. 1986, Nature, **319**, 205.

Eilek, J. A., and Kafatos, M. 1983, Ap. J., **271**, 804.

Gloeckler, G., and Jokipii, J. R. 1967, Ap. J., **148**, L41.

Golden, R. L., Horan, S., Mauger, B. G., Badhwar, G. M., Lacy, J. L., Stephens, S. A., Daniel, R. R., and Zipse, J. E. 1979, Phys. Rev. Lett., **43**, 1196.

Golden, R. L. 1984, Proc. 19th Rencontre de Moriond Ap. Meeting, p. 193.

Gould, R. J. 1986, Nucl. Phys., **B266**, 737.

Hillas, A. M. 1984a, Ann. Rev. Astr. Ap., **22**, 425.

Hillas, A. M. 1984b, Nature, **312**, 50.

Jacobson, A. S., Ling, J. C., Mahoney, W. A., and Willett, J. B. 1978, in Gamma Ray Spectroscopy in Astrophysics, ed. T. L. Cline and R. Ramaty (NASA TM 79619), p. 228.

Kazanas, D., and Ellison, D. C. 1986, Nature, **319**, 380.

Kolykhalov, P. I. and Sunyaev, R. A. 1979, Sov. Astr., **23**, 189.

Ling, J. C., Mahoney, W. A., Willett, J. B., and Jacobson, A. S. 1983, in Gamma Ray Transients and Related Astrophysical Phenomena, ed. R. E. Lingenfelter, H. S. Hudson, and D. M. Worrall (AIP: New York), p. 143.

Mahoney, W. A., Ling, J. C., Wheaton, W. A., and Jacobson, A. S. 1984, Ap. J., **286**, 573.

Meszaros, P. 1983, Ap. J., **274**, L13.

Meszaros, P., and Ostriker, J. P. 1983, Ap. J., **273**, L59.

Murphy, R. J. 1985, Ph. D. Thesis, Univ. of Maryland.

Murphy, R. J., and Ramaty, R. 1985, Adv. Space Res., **4**,127.

Murphy, R. J., Dermer, C. D., and Ramaty, R. 1987, Ap. J. (Suppl.), submitted.

Petrosian, V., and Ramaty, R. 1972, Ap. J., **173**, L83.

Ramaty, R., Kozlovsky, B., and Lingenfelter, R. E. 1975, Space Sci. Rev., **18**, 341.

Ramaty, R. and Meszaros, P. 1981, Ap. J., **250**, 384.

Shapiro, S. L., Lightman, A. P., and Eardley, D. M. 1976, Ap. J., **204**, 187.

Stephens, S. A. 1981, Ap. and Space Sci., **76**, 87.

Tan, L. C., and Ng, L. K. 1983a, J. Phys. G, **9**, 1289.

Tan, L. C., and Ng, L. K. 1983b, J. Phys. G, **9**, 227.

Vestrand, W. T. and Eichler, D. 1982, Ap. J., **261**, 251.

Wang, H. T., and Ramaty, R. 1974, Solar Phys., **36**, 129.